

SEPARATE INTEGRATION OF SOLAR PVS INTO THE LOW-VOLTAGE DC LINK OF A SOLID-STATE TRANSFORMER BASED ON A MODULAR MULTILEVEL CONVERTER

AHMED FAROUK KASSE, NADIR KABECHE, SAMIR MOULAHOUIM

Keywords: Photovoltaic power systems; Solid-state transformer; DC-DC converter; Modular multilevel converter.

This paper presents a photovoltaic system connected to a solid-state transformer (SST). The PVs are integrated into the low-voltage DC (LVDC) link. The SST consists of three stages containing combinations of converters: the modular multilevel converter MMC is employed in the medium voltage (LV) stage, the DC-DC converter is applied in the isolated stage, and a three-phase inverter is utilized in the low voltage (LV) stage. To ensure the smooth integration of PVs, it is essential to maintain a stable voltage at the LVDC level. To this end, the application control of the DC-DC converter must be used. The single-phase shift control (SPS) strategy was adopted. This control strategy maintains DC voltage levels at appropriate values and enables bidirectional power flow. In addition, to optimize the extraction of maximum power from the PVs, a maximum power point tracking (MPPT) technique is applied based on the M5P model decision tree. In parallel, to ensure optimal operation of the SST, a voltage-oriented control (VOC) and voltage capacitor balancing algorithm based on rotating gating signals is implemented for the MMC converter. In contrast, an unbalanced load control is applied to the inverter. The model developed in this study was implemented in MATLAB/Simulink, and the system's dynamic performance was validated.

1. INTRODUCTION

The growing need for renewable energy is emerging because of increased demand for electricity and growing environmental concerns about fossil fuel sources. This has contributed to the rapid spread of grid integration of photovoltaic power plants. The solid-state transformer (SST) is considered a suitable option for solar system integration due to its superior power quality, density, efficiency, and additional control capabilities. The various topologies of the SST have been extensively discussed in several scientific papers [1,2].

SST is a combination of electronic power converters and a high-frequency transformer that uses link voltage stages isolated from each other. Like the ordinary characteristics of conventional transformers, which include voltage matching and galvanic isolation, the SST improves the power supply system by enabling control of voltage and power, connected devices, and real-time monitoring. Additionally, the SST offers several benefits, including bidirectional power flow, reduced size and weight, high energy density, a small number of passive components, and DC voltage outputs [3,4]. The standard SST design has three stages: a rectifier at the input, a high-frequency DC/DC converter, and a three-phase inverter at the output [5–7].

In the context of medium-voltage (MV) distribution grids, it is essential to consider the multi-level configuration within the SST. Various multilevel inverter configurations have been proposed to meet the requirements of SST applications [8]. Integrating the modular multilevel converter (MMC) has attracted considerable interest in high and medium-voltage applications. The inherent advantages of the MMC exceed those offered by conventional topologies, notably its modular design, allowing flexibility in the creation of varied voltage levels through the addition of sub-modules. A key feature is its ability to attenuate low-frequency harmonics resulting from switching, which reduces switching losses.

Furthermore, to guarantee optimal MMC operation, keeping the capacitor voltages within the sub-modules (SMs) stable and balanced is imperative, in line with their nominal values. Achieving this objective requires using a voltage-balancing algorithm, an aspect addressed in previously published work [9–11], which presented various strategies

for balancing capacitor voltages. The voltage balancing approach utilized in this study is based on rotating gating signals between the sub-modules [12].

In photovoltaic (PV) system applications, maximum power extraction is problematic under undesirable conditions such as irregular radiation, temperature, partial shading, and dust accumulation. Several topologies have been proposed in the publication to achieve the best performance and requirements for grid-connected PVs [13,14]. Therefore, the SST is an excellent solution for integrating PVs using different methods. Additionally, The SST includes a DC link that permits the direct integration of PVs into the grid; this will facilitate the direct connection of PVs to the SST, which can significantly improve the performance. This paper has integrated PVs with the SST's low-voltage (LVDC) link. This is achieved separately. This methodology offers several considerable advantages. Firstly, it simplifies the connection process by eliminating complex intermediate steps.

What's more, this configuration facilitates the establishment of bidirectional power flow. However, to ensure stable integration, it is essential to implement control for the DC-DC converter. This controller maintains DC voltage levels at appropriate levels. The single-phase shift control (SPS) is used for the DC-DC converter. Furthermore, a maximum power point tracking (MPPT) approach is imperative to optimize power extraction from the PVs. Several MPPT control techniques have been explored in the literature [15,16]. However, these conventional MPPT methods have exhibited inherent drawbacks, such as susceptibility to fluctuating environmental conditions.

Additionally, integrating the PVs with the LVDC link of the SST exacerbates power and output voltage response fluctuations within a boost converter. Consequently, these limitations restrict the overall power extraction efficiency of the PVs. A maximum power point tracking technique based on the M5P tree addresses these challenges. The M5P tree represents a machine-learning model known as a decision tree, specifically a regression tree. In this MPPT approach, the MPPT collects the input data using fuzzy logic. This combined control capitalizes on both the reasoning advantages of fuzzy logic and the fast and accurate processing functionality of the M5P tree [17]. This strategy

exhibits exceptional efficacy, even when the PVs operate under dynamic conditions. In addition, a series of control strategies have been introduced to ensure optimum stability and operation of the overall system. On the MV side, a voltage-oriented control (VOC) technique and a voltage balancing approach are deployed to maintain the balance of the MMC capacitors. An unbalanced control load was used for the inverter on the SST's low-voltage (LV) side. The proposed architecture with its controllers is simulated in the MATLAB/Simpower environment. The simulated results attest to the effectiveness of this architecture for integrating photovoltaic systems.

The structure of this study is as follows: section 2 discusses in detail the proposed configuration of the PVs integrated with the SST, while section 3 goes into more detail on the design of the SST and aspects relating to its control. Subsequently, section 4 presents the simulation results and offers a concrete validation of the approach adopted. Finally, the conclusions of the study are summarized in section 5.

2. SYSTEM CONFIGURATION

The optimal PV integration option is the three-stage SST based on a dual-active-bridge (DAB) converter. Considering the advantages of bidirectional power flow, this structure is built on the LVDC link for PVs. In this studied system, the phase shift angle between two stages controls the PV side voltage, but the power flow is always unidirectional. This paper uses a three-phase SST topology using MMC technology to integrate the PVs on the LVDC link in a separate way. This method allows us to take advantage of the LVDC link of the SST to insert the PV power into the MV grid. This innovative approach enables bidirectional power flow and enhances the overall performance and flexibility of the system. The system architecture shown in (Fig. 1) includes solar arrays connected separately with the LVDC link of the SST. The SST consists of three stages. The first

stage is the medium-voltage stage, where a three-phase MMC rectifies the AC medium voltage to a DC voltage. The second stage is the isolated DC-DC stage, which consists of two converters and a high-frequency transformer (HFT). Where the dynamics of power transfers are based on the square wave. Finally, the third stage is a three-phase inverter providing a low alternating load current. In addition, the PV stage consists of PV arrays and boost converters.

3. SYSTEM OPERATION AND CONTROL

Figure 2 shows the schematic of the MMC control diagram. The MMC consists of three phases, each comprising both upper and lower arms with inductors and four SMs in series. Each half-bridge SM comprises a capacitor coupled to two IGBTs with complementarily switching. The VOC method is used to supply single references for the PWM generator. The VOC control enables the elimination of harmonics, the resolution of the circulating current issue, and the power factor optimization. PWM uses the PSC-PWM technique with phase-shifted triangular signals to regulate the submodules. The mathematical analyses and control of the MMC are provided in [18–21].

Furthermore, the capacitor voltage balancing algorithm plays an essential role in the correct operation and reliability of the MMC. It aims to maintain equal voltage levels between the capacitors connected to the SMs, thus ensuring a balanced distribution of electrical loads. This voltage equality is crucial to avoid imbalances that could cause performance and stability problems in the system. The algorithm uses rotating gating signals between the submodules to achieve voltage balancing. In practical terms, this means that specific combinations of switching between sub-modules are chosen depending on the current direction and capacitor charge/discharge conditions. These combinations control how charges are distributed between capacitors, enabling voltage levels to be precisely adjusted [22].

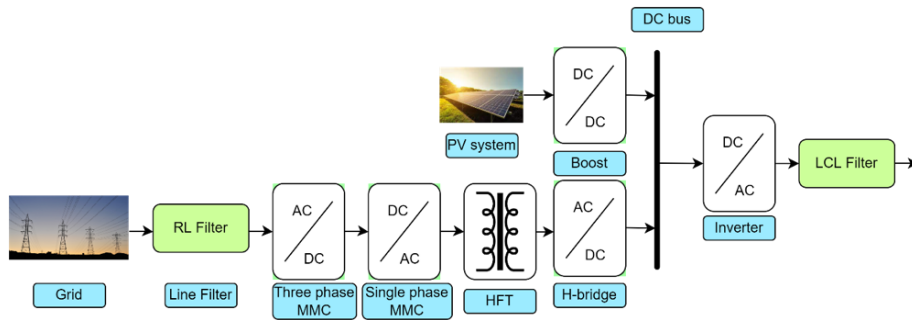


Fig. 1 – General system schematic configuration.

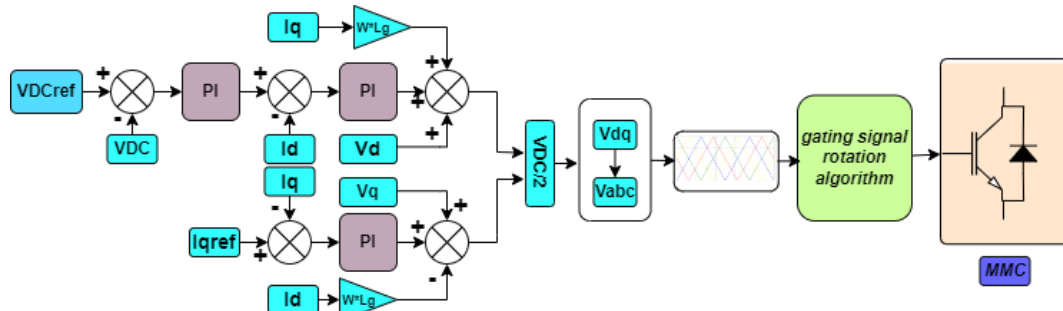


Fig. 2 – Three-phase MMC control diagram.

3.2. DC-LINK VOLTAGE CONTROL

Integrating PVs with SST in the LVDC link requires a synergistic combination of control strategies to ensure bidirectional power flow. In this configuration, the DC-DC converter is controlled using an SPS approach, while the PV's efficiency is optimized using MPPT methods.

By integrating the PVs at the LVDC link, DC link control is essential to enhance bidirectional power flow. To achieve this goal, the single-phase shifting approach was implemented. This precise control over the phase angle between the primary and secondary sides enables power transmission from the PVs to the grid and vice versa. Figure 3 depicts the basic schematic of the controller diagram. The output DC link voltage is compared with its reference value, and the resulting errors are sent to a PI controller. This signal is given into a delay angle generator. The delay angle generator provides the phase shift. In addition, this output signal generates the value of reference for the PWM block [23,24].

In the context of integrating the PVs into the LVDC link of the SST, it is crucial to establish efficient MPPT) to optimize energy extraction from the PVs. Traditional methods such as the P&O method and the fuzzy Fuzzy-MPPT approach are limited in their ability to extract maximum energy from the PVs due to the process of connecting the system PV to the LVDC link, which generates fluctuations in the voltage and current from the PV panels, hindering the extraction of the maximum available energy. To solve this problem, an approach based on the M5P tree was implemented for MPPT tracking. This M5P tree method presents a convincing alternative, as it takes advantage of fuzzy logic's reasoning capabilities and the fast, accurate processing capabilities specific to the M5P tree algorithm. This MPPT approach, therefore, proves to be a robust and effective solution for optimizing the energy extraction of the PVs.

The M5P algorithm is a decision tree-based machine learning algorithm for regression tasks. It is an extension of the traditional decision tree algorithm that aims to improve performance, especially when dealing with continuous or numeric target variables. Like conventional decision trees, the M5P can introduce a linear regression to the classical model according to specific parameters. The aim is to construct a learning model that can be used to predict the target value (terminal node) by teaching simple rules inferred from prior collected datasets.

The WEKA software tool is utilized to implement this tracking method. WEKA is a comprehensive suite of open-source machine-learning software designed to conduct tasks related to machine learning and classification. The procedure commences by collecting input and output data from the fuzzy-MPPT algorithm within the MATLAB/Simulink environment. Subsequently, these data are subjected to processing within the MATLAB/Simulink environment. The subsequent step entails converting the accumulated data into an Excel file format with a .ARFF extension, which is subsequently imported into the WEKA software. The steps to initiate a learning operation within the WEKA software are as follows: Go to Explorer. Choose the file data .arff (ARFF is an extension of WEKA files). Open Classify. Select the desired algorithm (in our case, M5P). Commence the learning operation. In the final step, the model derived from WEKA can be conveniently translated into MATLAB code with IF-ELSE instruction. A graphical representation of

this methodology (Fig. 4) illustrates the approach taken to obtain the final MATLAB program [25].

3.3. OUTPUT INVERTER STRUCTURE AND CONTROL

On the LV side of the SST, a three-phase inverter with an LCL coupled to the loads is used. A unified control strategy for the inverter has been proposed. The suggested controller allows the inverter to work under generalized unbalanced operating conditions. Moreover, the load voltage is automatically regulated, and the load current waveform quality is improved. This leads to keeping the harmonic content in applicable accepted terms and maintaining a near unity power factor. For further information about the control strategy elected for this inverter, see [26,27].

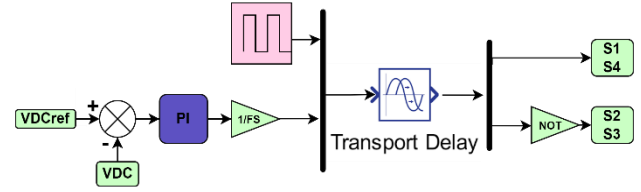


Fig. 3 – Single-phase bridge control diagram.

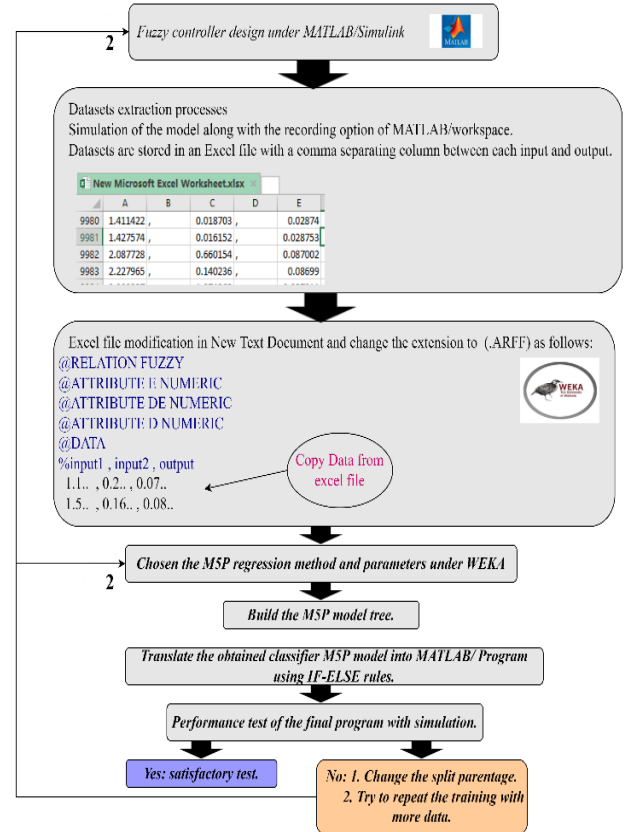


Fig. 4 – Research methodology to build the Matlab code.

4. SIMULATION AND RESULTS VALIDATIONS

The results of PVs connected to the SST within the LVDC link are presented using MATLAB/Simulink with a sampling time of 2 s. The specific parameters of the SST are listed in Table 1. The system operates with a rated power of 100 kVA, an input voltage of 1 kV between phases, a frequency of 50 Hz, and a power generated by the PV system of 25 kW. To evaluate system performance and observe

power flows between the grid, the load, and the photovoltaic generators, a variation in load power was applied at $t = 0.8$ s and irradiation conditions at $t = 1.5$ s.

Figure 5 elucidates the power output dynamics from the grid, loads, and PVs. It is discernible that when the load requires high power (70 kW), PVs continue to generate their full output of 25 kW, while the grid supplies the remaining power (45 kW). When the load decreases to 15 kW, the PVs persist in producing 25 kW, indicating that the excess 10 kW is being returned to the grid. This corresponds to the behavior in which grid power reduces significantly from about 45 kW to nearly zero. Moreover, while the production of PVs declines due to decreased irradiation, grid power increases, offering additional support to satisfy the reduced load demand. However, the sum of the powers does not appear perfectly balanced due to inherent system losses and transient dynamics. Losses in the elements of the MMC, such as arm resistors, SM capacitors, and arm inductors, consume a part of power that is not shown in the figure. In addition, low-voltage DC link capacitors temporarily store or release energy during transitions, causing short-term power imbalances. Despite these factors, the system achieves a stable overall balance, where the load is continuously satisfied and excess PVs are efficiently managed, proving the effectiveness of the proposed control strategies.

Figure 6 offers insights into the stability of the medium and low side DC voltages, underscoring their constancy at reference values. The observed stability at the LVDC link validates the efficacy of the implemented control strategies, particularly emphasizing the success of the phase shift control technique in maintaining voltage stability.

Table 1
System parameter

Parameters	Value
Filter grid Resistance (R_g)	0.05 Ω
Filter grid inductance (L_g)	0.0032 H
MMC SM capacitor (C_{sm})	0.0025 F
MMC Arm resistance (R_{arm})	10 Ω
MMC Arm inductance (L_{arm})	0.8 mH
DC link capacitor (C_{dc})	0.0019 F
R_{arm} of single-phase MMC	0.2 Ω
L_{arm} of single-phase MMC	0.025 mH
C_{sm} of single-phase MMC	0.002 F
The leakage inductance	0.0025 mH
DC link capacitor LV side	0.003 F

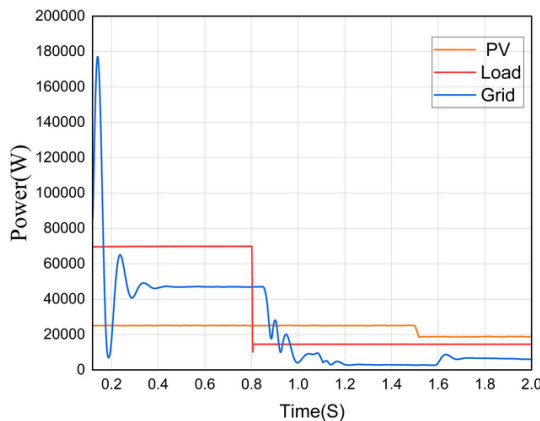


Fig. 5 – Powers of grid and load and PV arrays.

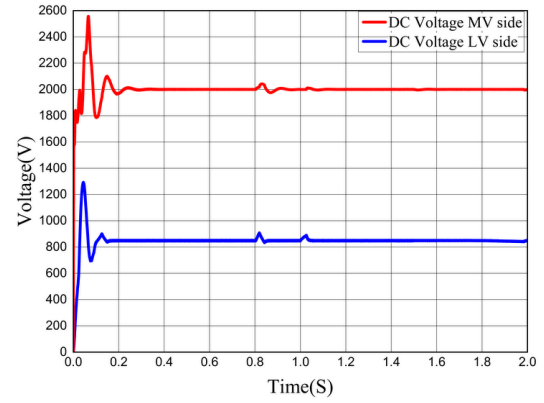


Fig. 6 – DC Voltage at the output MV and LV.

The voltage and current of the PVs are shown in Fig. 7. The voltage is stable but with visible oscillations and is most apparent at the current. These oscillations may be traced back to the MPPT algorithm's dynamic reaction. However, using the M5P decision tree-based MPPT greatly minimizes the size of these oscillations. This is due to the M5P algorithm's more accurate prediction of the MPP and ability to stabilize the system without adding additional disturbances. Despite the reduction in oscillation frequency and amplitude, some residual variations remain.

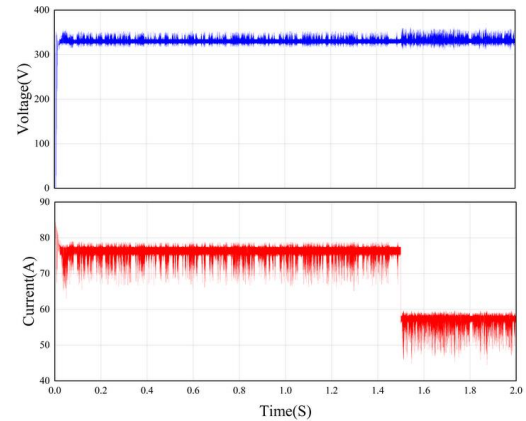


Fig. 7 – Voltages and currents of the PV arrays.

Figure 8 offers insights into the stability of the medium and low side DC voltages, underscoring their constancy at reference values. The observed stability at the LVDC link validates the efficacy of the implemented control strategies, particularly emphasizing the success of the phase shift control technique in maintaining voltage stability.

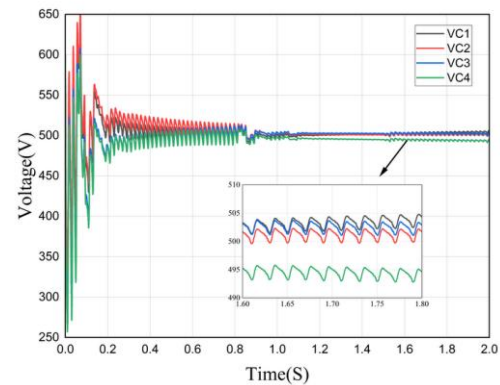


Fig. 8 – The capacitor voltage of an arm of the MMC.

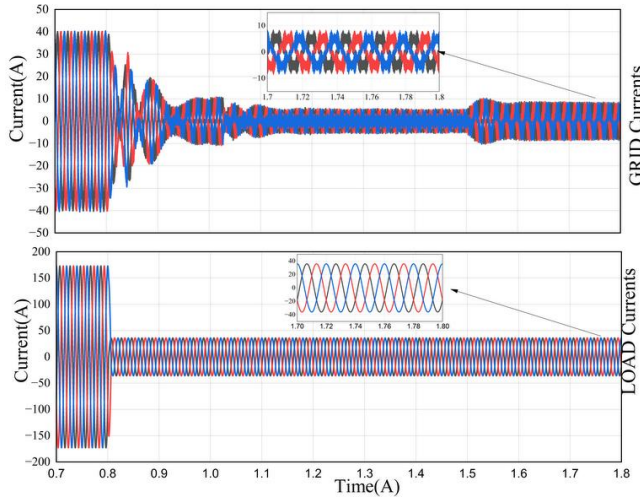


Fig. 9 – Currents of the grid and the loads.

Figure 9 illustrates the grid and load currents' behavior. Initially, the grid currents exhibit high oscillations due to transient interactions within the system. The system stabilizes the currents and reduces these oscillations over time. However, the grid currents retain noticeable harmonic distortion rather than appearing perfectly sinusoidal, as seen between 1.6 and 1.8 seconds. The interaction between the PV system and the MMC is responsible for this behavior. Specifically, the PV system introduces a high-frequency switching ripple into the DC link. Also, the MMC control does a good job of balancing the voltages of the submodule capacitors and keeping the fundamental frequency stable. Still, it doesn't entirely fix the harmonics that the PV system creates. The load currents demonstrate a steady-state condition after the transient period, aligning with the expected sinusoidal nature of the system. Figure 10 presents the voltages for both the grid and the load. These voltage waveforms exhibit a similar sinusoidal profile, confirming the balance between load demand and grid supply.

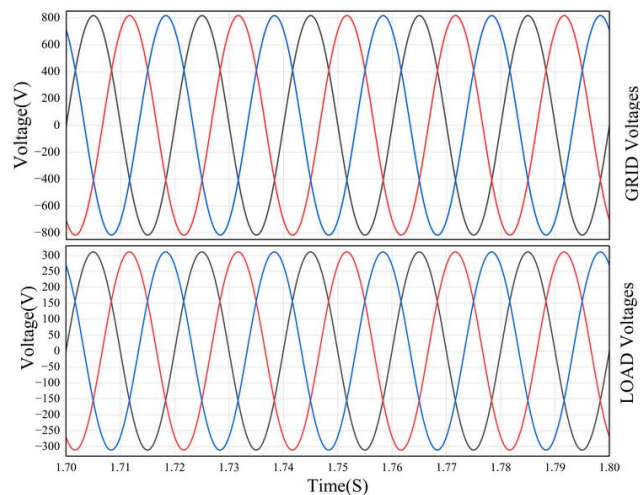


Fig. 10 – Voltages of the grid and the loads.

11. CONCLUSIONS

This paper integrated the PVs separately in the SST's low-voltage-DC (LVDC) link. The SST is a combined power converter. This method streamlines the connection process

and facilitates bidirectional power flow, thus simplifying PV integration. The SPS control ensures stable integration by regulating DC voltage levels appropriately. Additionally, the incorporation of MSP-MPPT maximizes power extraction from PV generators, ensuring optimal performance even under varying conditions.

Furthermore, the VOC technique, as well as a voltage balancing algorithm based on rotating gating signals, are employed to ensure the capacitor voltage balanced and optimal operation of the MMC, and an unbalanced load control for the LV-side inverter has been implemented to ensure optimal operation of the SST. The system was developed and implemented under MATLAB/Simulink. The simulation results demonstrate the effectiveness of the direct integration of the PVs in the LVDC link of the SST where the bidirectional power flow is achieved.

CREDIT AUTHORSHIP CONTRIBUTION STATEMENT

Kasse Ahmed Farouk: Methodology, Software, Validation, wrote the main manuscript.

Kabache Nadir: Investigation, Writing, Validation, Review.

Samir Moulahoum: Methodology, Investigation, Validation, Review.

Received on 4 December 2024

REFERENCES

1. S. Khan, K. Rahman, M. Tariq, S. Hameed, B. Alamri, T.S. Babu, *Solid-state transformers: fundamentals, topologies, applications, and future challenges*, Sustainability, **14**, 1, p. 1319 (2022).
2. D. Cervero, M. Fotopoulou, J. Muñoz-Cruzado, D. Rakopoulos, F. Stergiopoulos, N. Nikolopoulos, S. Voutetakis, J.F. Sanz, *Solid state transformers: a critical review of projects with relevant prototypes and demonstrators*, Electronics, **12**, 4, p. 931 (2023).
3. X. She, A.Q. Huang, R. Burgos, *Review of solid-state transformer technologies and their application in power distribution systems*, IEEE Journal of Emerging and Selected Topics in Power Electronics, **1**, 3, pp. 186–198 (2013).
4. D.K. Mishra, M.J. Ghadi, L. Li, M.J. Hossain, J. Zhang, P.K. Ray, A. Mohanty, *A review on solid-state transformer: a breakthrough technology for future smart distribution grids*, International Journal of Electrical Power & Energy Systems, **133**, pp. 107–255 (2021).
5. R. Gao, X. She, I. Husain, A.Q. Huang, *Solid-state-transformer interfaced permanent magnet wind turbine distributed generation system with power management functions*, IEEE Transactions on Industry Applications, **53**, 4, pp. 3849–3861 (2017).
6. X. She, X. Yu, F. Wang, A.Q. Huang, *Design and demonstration of a 3.6-kV-120-V/10-kVA solid-state transformer for smart grid application*, Transactions on Power Electronics, **29**, 8, pp. 3982–3997 (2014).
7. M.A. Hannan, P.J. Ker, M.S.H. Lipu, Z.H. Choi, M.S.Abd. Rahman, K.M. Muttaqi, F. Blaabjerg, *State of the art of solid-state transformers: advanced topologies, implementation issues, recent progress and improvements*, IEEE Access, **8**, pp. 19113–19132 (2020).
8. M.M.E. Adabi, J.A. Martinez-Velasco, S. Alepuz, *Modeling and simulation of a MMC-based solid-state transformer*, Electrical Engineering, **100**, 2, pp. 375–387 (2017).
9. L.A.M. Barros, A.P. Martins, J.G. Pinto, *A comprehensive review on modular multilevel converters, submodule topologies, and modulation techniques*, Energies, **15**, 3, p. 1078 (2022).
10. M. Priya, P. Ponnambalam, K. Muralikumar, *Modular-multilevel converter topologies and applications – a review*, IET Power Electronics, **12**, 1, pp. 1–15 (2019).
11. Q. Xi, Y. Tian, Y. Fan, *Capacitor voltage balancing control of MMC sub-module based on neural network prediction*, Electronics, **13**, 4, p. 795 (2024).
12. F. Gao, L. Xu, L. Zhang, *A rotating gating signal method for capacitor voltage balancing in modular multilevel converters*, IEEE Transactions on Power Electronics, **28**, 1, pp. 300–308 (2013).
13. S. Kouser, G.R. Dheep, R.C. Bansal, *Maximum power point tracking techniques for photovoltaic systems: a review*, Renewable and

- Sustainable Energy Reviews, **159**, pp. 112–123 (2023).
14. V.G. Dogaru, F.D. Dogaru, V. Năvrăpescu, L.M. Constantinescu, *From the photovoltaic effect to a low voltage photovoltaic grid challenge –a review*, Rev. Roum. Sci. Techn. –Electrotechn. et Energ., **69**, 3, pp. 263–268 (2024).
 15. M.L. Katche, A.B. Makokha, S.O. Zachary, M.S. Adaramola, *A comprehensive review of maximum power point tracking (MPPT) techniques used in solar PV systems*, Energies, **16**, 5, p. 2206 (2023).
 16. Y.K. Teklehaimanot, F.K. Akingbade, B.C. Ubochi, T.O. Ale, *A review and comparative analysis of maximum power point tracking control algorithms for wind energy conversion systems*, International Journal of Dynamics and Control, **12**, pp. 3494–3516 (2024).
 17. S.A. Blaifi, S. Moulahoum, R. Benkercha, B. Taghezouit, A. Saim, *MSP model tree-based fast fuzzy maximum power point tracker*, Solar Energy, **163**, 15, pp. 405–424 (2018).
 18. R. Teodorescu, L. Zarri, *Modular multi-level converter: modeling, simulation, and control in steady state and dynamic conditions*, Aalborg University, 2012.
 19. M. Hagiwara, H. Akagi, *Control and experiment of pulse width-modulated modular multilevel converters*, IEEE Transactions on Power Electronics, **24**, 7, p. 1737–1746 (2009).
 20. R. Darus, J. Pou, G. Konstantinou, S. Ceballos, R. Picas, V.G. Agelidis, *A modified voltage balancing algorithm for the modular multilevel converter: evaluation for staircase and phase-disposition PWM*, IEEE Transactions on Power Electronics, **30**, 1, pp. 298–310 (2015).
 21. W. Luo, Y. Ma, C. Zheng, *Selection-based capacitor voltage balancing control for modular multilevel converters*, Journal of Power Electronics, **21**, pp. 1427–1438 (2021).
 22. G.P. Adam, O. Anaya-Lara, G.M. Burt, D. Telford, B.W. Williams, J.R. McDonald, *Modular multilevel inverter: pulse width modulation and capacitor balancing technique*, IET Power Electronics, **3**, pp. 702–715 (2010).
 23. M. Alshammari, M. Duffy, *Review of single-phase bidirectional inverter topologies for renewable energy systems with DC distribution*, Energies, **15**, 18, p. 683 (2022).
 24. F. Jarraya, A. Khan, A. Gastli, L. Ben-Brahim, R. Hamila, *Design considerations, modelling, and control of dual-active full bridge for electric vehicles charging applications*, Journal of Engineering, **19**, 1, p. 5279 (2019).
 25. A. Bouhounta, S. Moulahoum, N. Kabache, *A novel combined Fuzzy-MSP model tree control applied to grid-tied PVs with power quality consideration*, Energy Sources, Part A: Recovery, Utilization, and Environmental Effects, **44**, 2, pp. 3125–3147 (2022).
 26. Y. Li, J. Zhang, Z. Hao, P. Tian, *Improved PR control strategy for an LCL three-phase grid-connected inverter based on active damping*, Applied Sciences, **11**, 7, p. 3170 (2021).
 27. J. Almaguer, V. Cárdenas, A. Aganza-Torres, M. González, J. Alcalá, *A frequency-based LCL filter design and control considerations for three-phase converters for solid-state transformer applications*, Electrical Engineering, **101**, pp. 545–558 (2019).